Supporting Information for

Mixed-dimensional self-assembly organic-inorganic perovskite microcrystals for stable and efficient photodetectors

Yunuan Wang, Yang Tang, Jingzan Jiang, Quan Zhang, Jun Sun, Yufeng Hu, Qiuhong Cui, Feng Teng, Zhidong Lou,* and Yanbing Hou*

Key Laboratory of Luminescence and Optical Information, Ministry of Education, Beijing Jiaotong University, Beijing 100044, China.
Email addresses: zhdlou@bjtu.edu.cn, and ybhou@bjtu.edu.cn

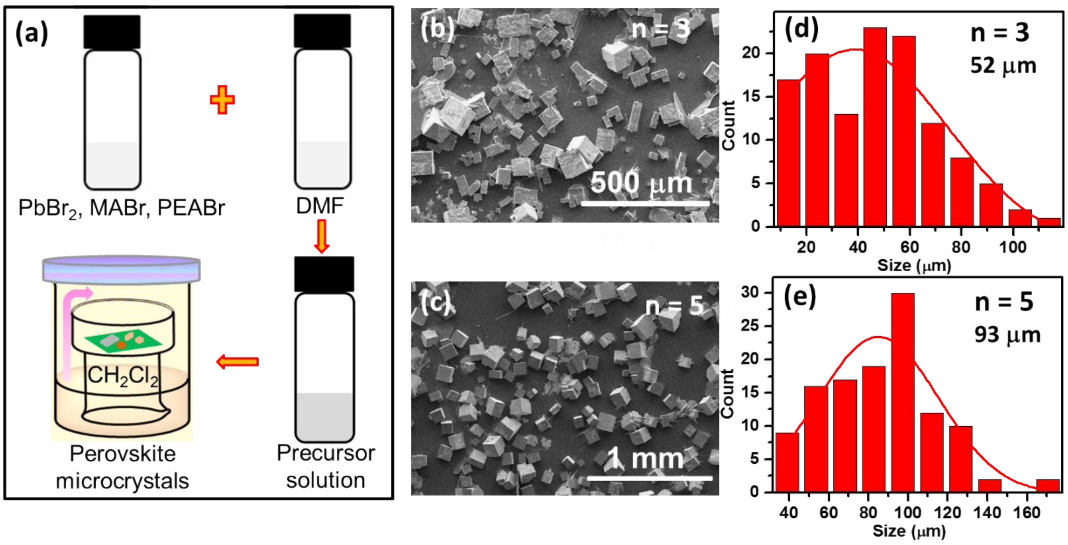

Fig. S1 (a) Schematic of the synthesis procedure for the $(PEA)_2(MA)_{n-1}Pb_nBr_{3n+1}$ (n = 1, 3, 5, ∞) perovskite microcrystals by an anti-solvent vapor-assisted method (ASV). The entire setup was sealed with tin foil and stood for 24 h at room temperature in air. (b), (c) Top-view SEM images and (d), (e) the corresponding size distributions of the cubes in the $(PEA)_2(MA)_2Pb_3Br_{10}$ and $(PEA)_2(MA)_4Pb_5Br_{16}$ perovskite microcrystals, respectively.

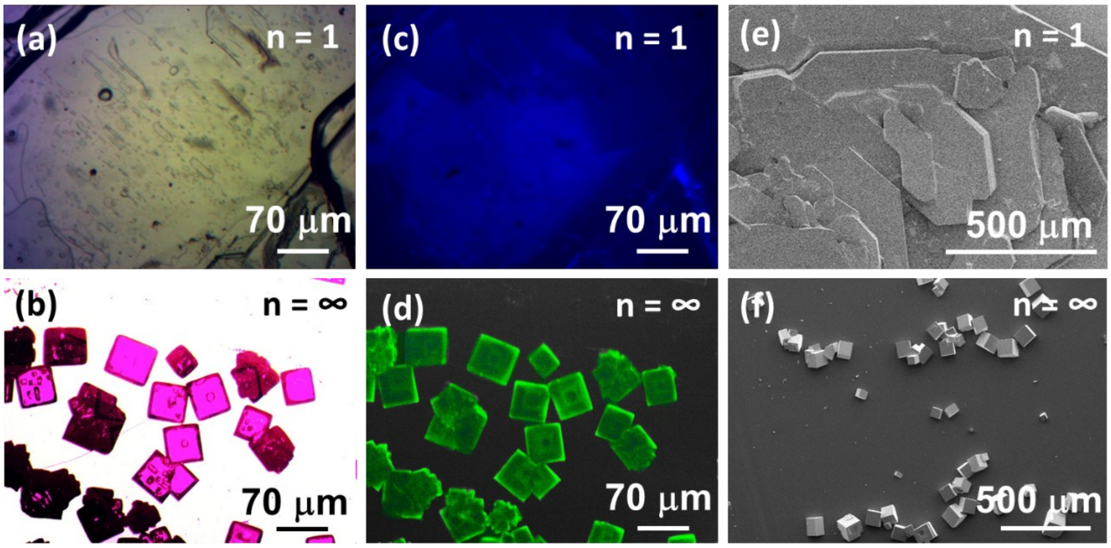

Fig. S2 (a), (b) Optical microscope images, (c), (d) fluorescence microscope images, and (e), (f) top-view SEM images of the $(PEA)_2PbBr_4$ and $MAPbBr_3$ perovskite microcrystals, respectively.

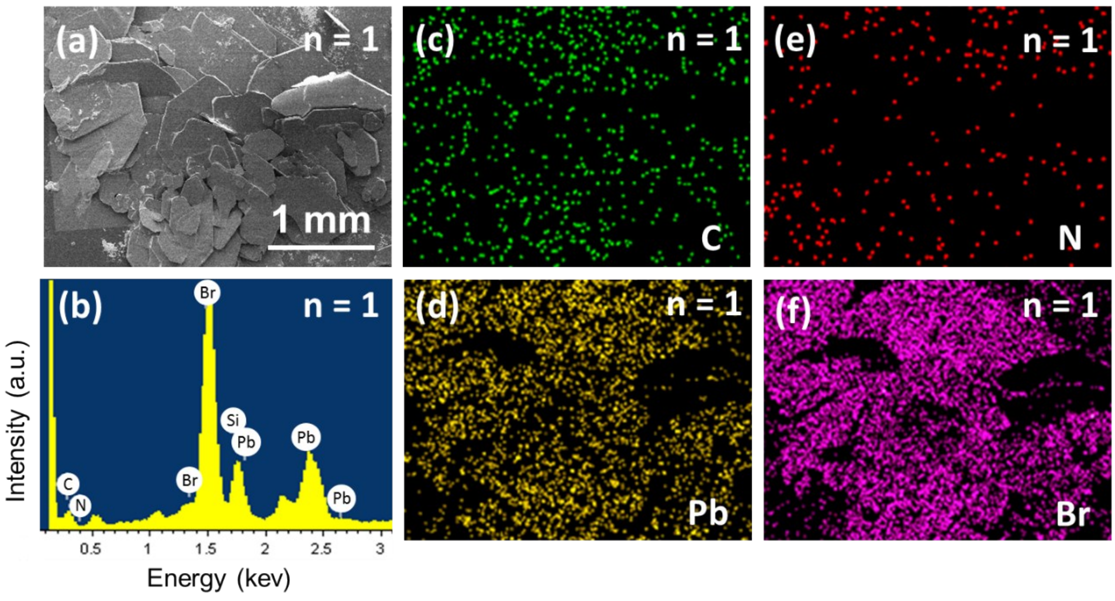

Fig. S3 (a) SEM image, (b) EDS spectrum, and (c)-(f) the corresponding EDS elemental mappings of the $(PEA)_2PbBr_4$ microcrystals.

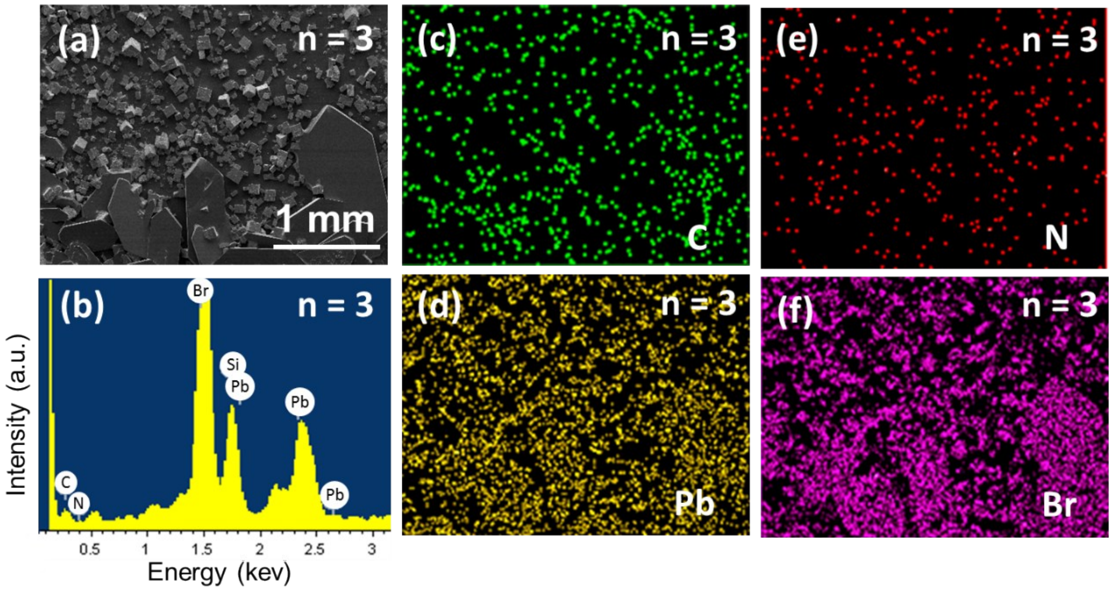

Fig. S4 (a) SEM image, (b) EDS spectrum, and (c)-(f) the corresponding EDS elemental mappings of the $(PEA)_2(MA)_2Pb_3Br_{10}$ perovskite microcrystals.

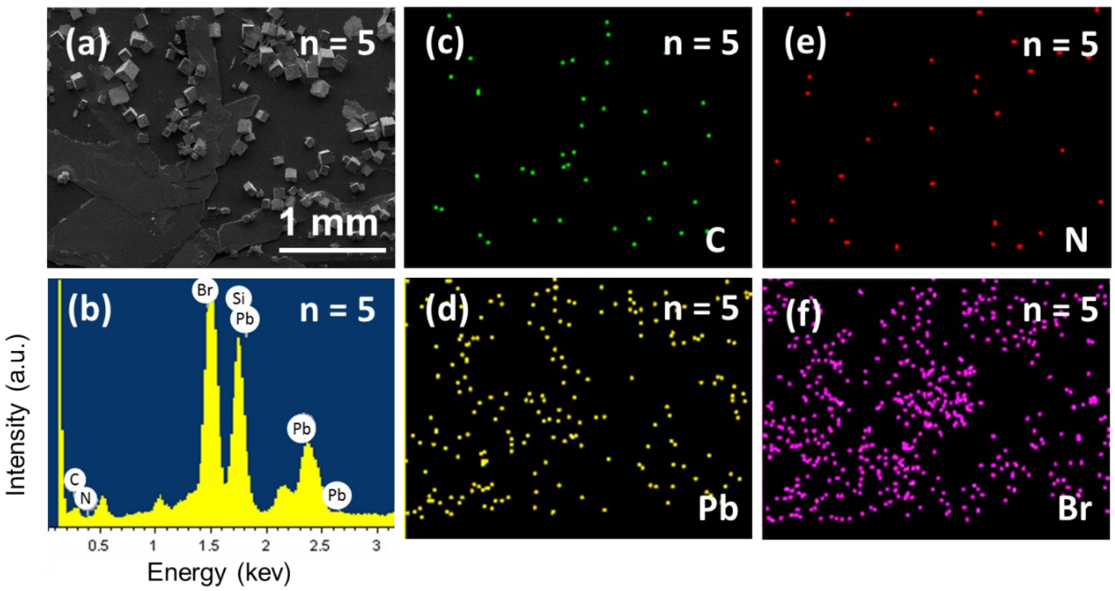

Fig. S5 (a) SEM image, (b) EDS spectrum, and (c)-(f) the corresponding EDS elemental mappings of the $(PEA)_2(MA)_4Pb_5Br_{16}$ perovskite microcrystals .

.

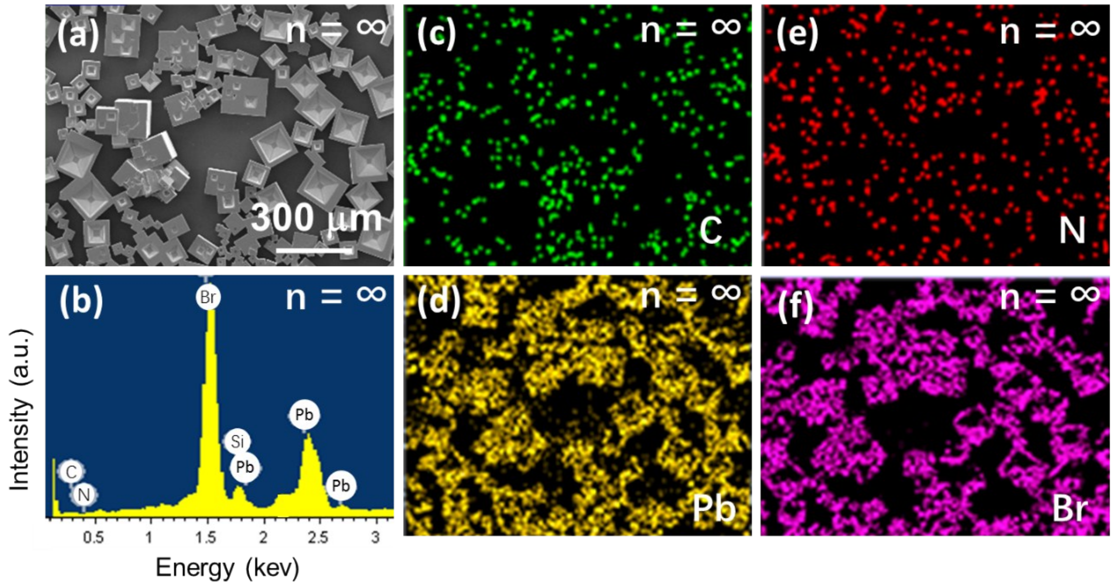

Fig. S6 (a) SEM image, (b) EDS spectrum, and (c)-(f) the corresponding EDS elemental mappings of the $MAPbBr_3$ microcrystals.

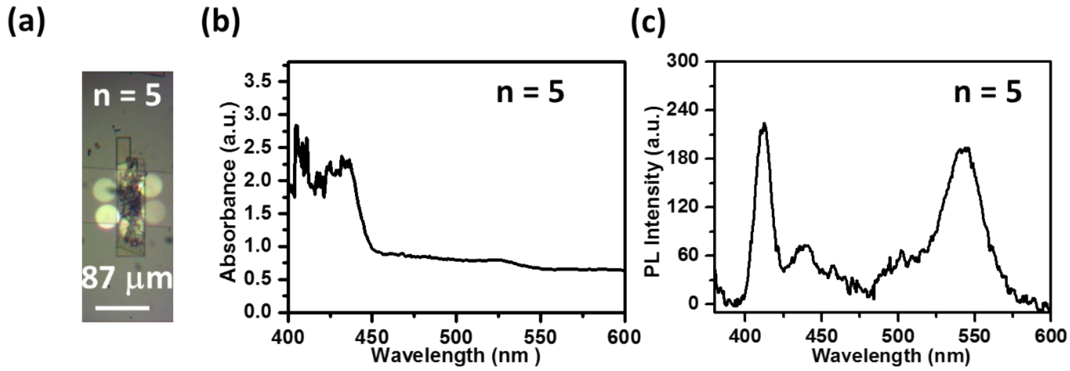

Fig. S7 (a) Optical microscope image, (b) micro-area absorption spectrum, and (c) micro-area PL spectrum of the $(PEA)_2(MA)_4Pb_5Br_{16}$ perovskite microcrystal photodetector. The center position in (a) surrounded by six bright spots is the test area.

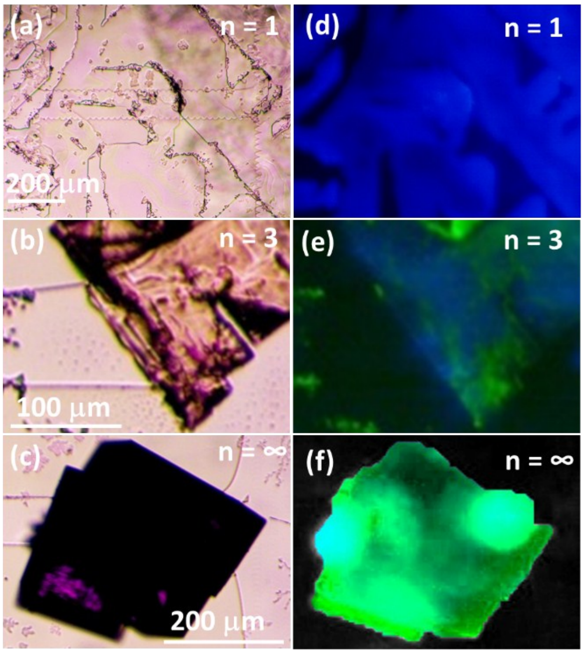

Fig. S8 (a), (b), (c) Optical microscope images and (d), (e), (f) fluorescence microscope images of the photodetectors based on the $(PEA)_2PbBr_4$, $(PEA)_2(MA)_2Pb_3Br_{10}$, and $MAPbBr_3$ perovskite microcrystals, respectively.

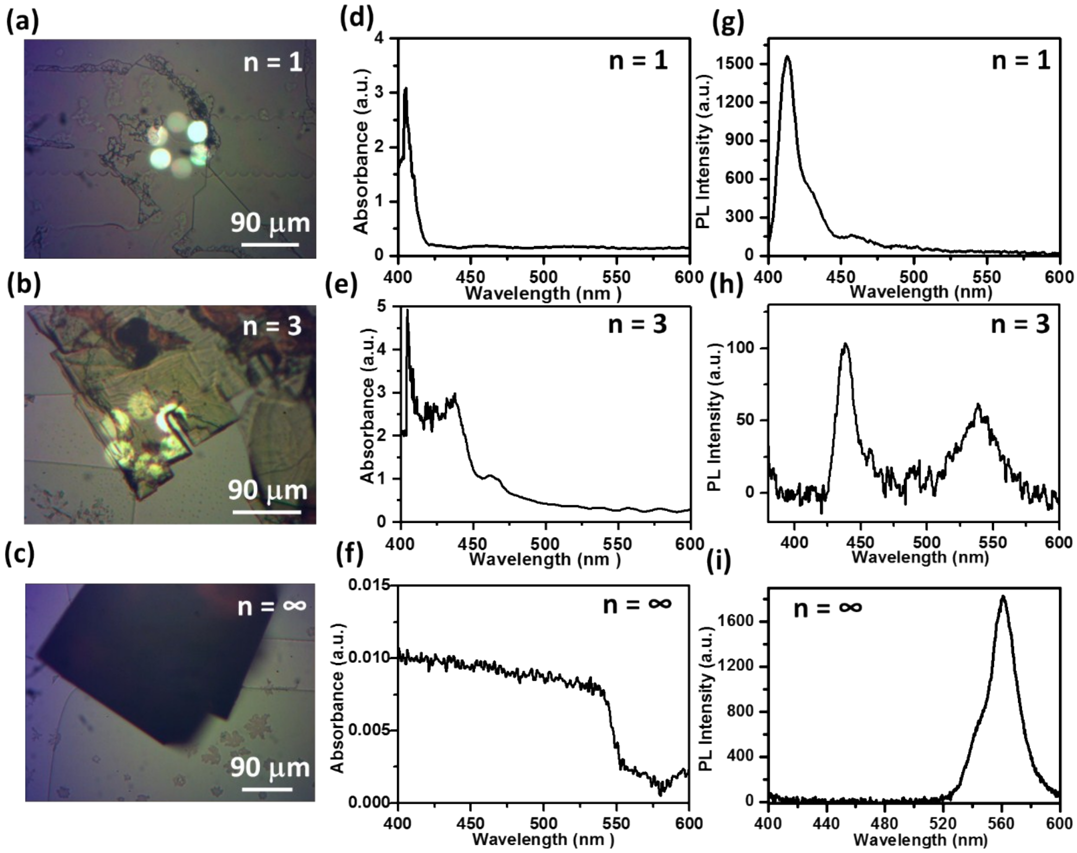

Fig. S9 (a), (b), (c) Optical microscope images, (d), (e), (f) micro-area absorption spectra, and (g), (h), and (i) micro-area PL spectra of the $(PEA)_2PbBr_4$, $(PEA)_2(MA)_2Pb_3Br_{10}$, and $MAPbBr_3$ perovskite microcrystal photodetectors, respectively. The center positions surrounded by six bright spots in (a), (b), (c) are the test areas. The spots in (c) are invisible since the $MAPbBr_3$ microcube is much thicker.

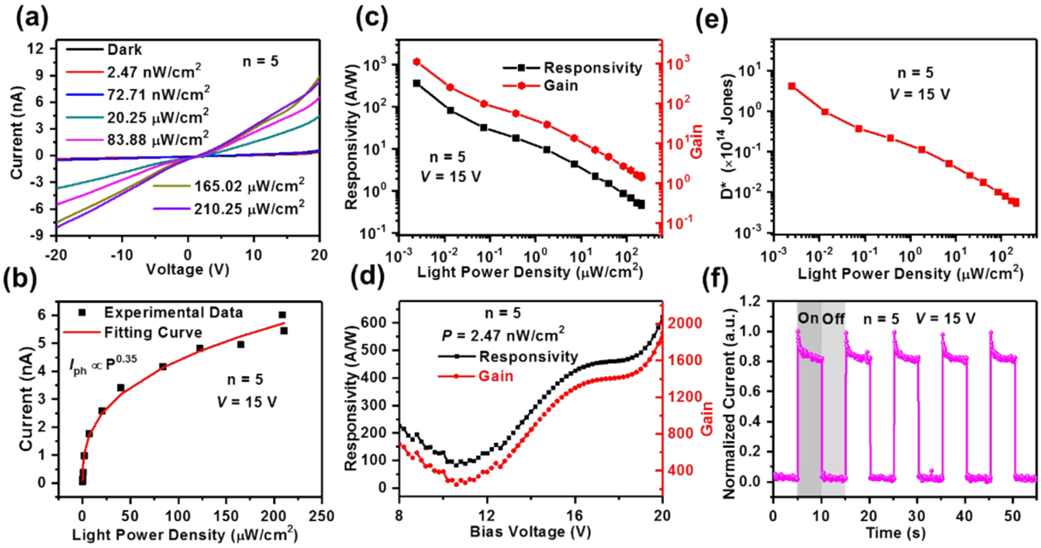

Fig. S10 Device stability of the mixed-dimensional $(PEA)_2(MA)_4Pb_5Br_{16}$ perovskite microcrystal photodetector. The following characteristics were investigated after the photodetector was placed in an atmospheric environment with a humidity of 60% for 8 days. (a) *I-V* characteristics of the photodetector in the dark and under 405-nm light illumination at various power intensities. (b) Photocurrent as a function of light intensity at 15 V. (c) Variations of responsivity and gain with light intensity at 15 V. (d) Variations of responsivity and gain with voltage under a light intensity of 2.47 nW/cm^2. (e) Specific detectivity as a function of light intensity at 15 V. (f) Time-resolved response of the photodetector illuminated by 405-nm light pules at 5 s intervals at 15 V.

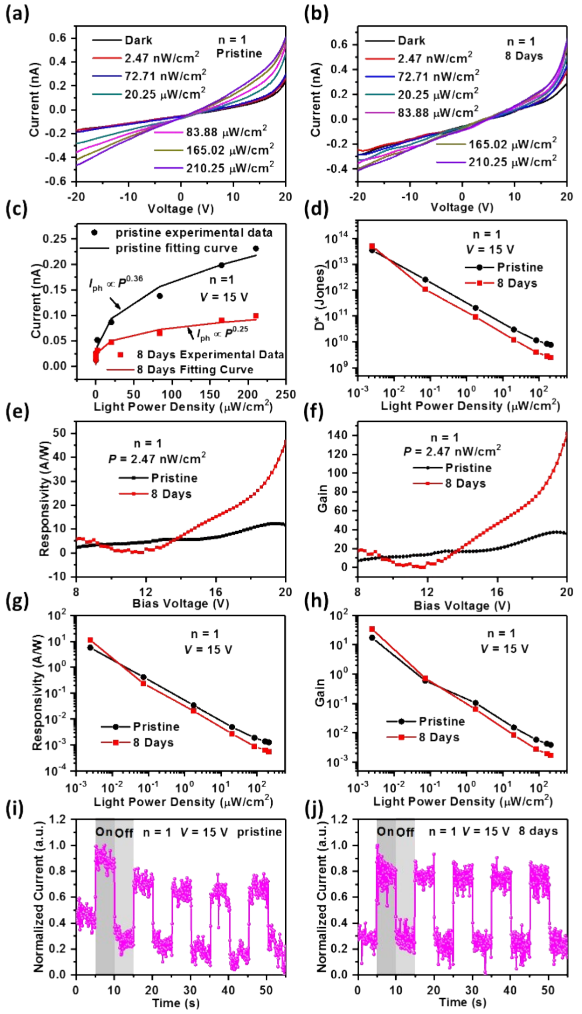

Fig. S11 Device characteristics of the pristine $(PEA)_2PbBr_4$ perovskite microcrystal photodetector and after being placed in an atmospheric environment with a humidity of 60% for 8 days. (a), (b) *I-V* characteristics in the dark and under 405-nm light illumination at various power intensities. (c), (d) Variations of photocurrent and specific detectivity with light intensity. (e), (f) Variations of responsivity and gain with voltage under a light intensity of 2.47 nW/cm^2. (g), (h) Variations of responsivity and gain with light intensity at 15 V. (i), (j) Time-resolved response of the photodetector illuminated by 405-nm light pules at 5 s intervals at 15 V.

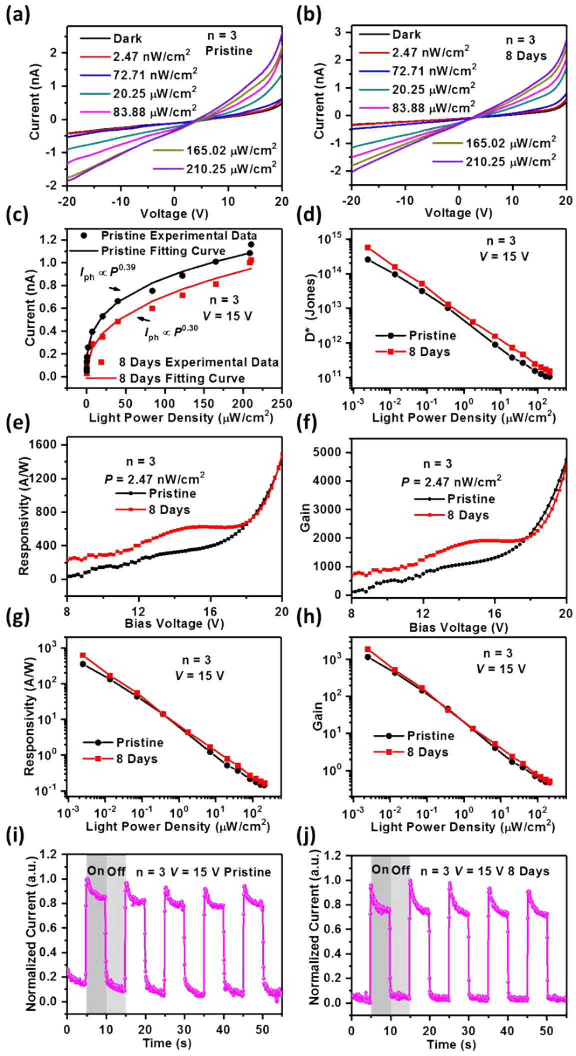

Fig. S12 Device characteristics of the pristine $(PEA)_2(MA)_2Pb_3Br_{10}$ perovskite microcrystal photodetector and after being placed in an atmospheric environment with a humidity of 60% for 8 days. (a), (b) *I-V* characteristics in the dark and under 405-nm light illumination at various power intensities. (c), (d) Variations of photocurrent and specific detectivity with light intensity at 15 V. (e), (f) Variations of responsivity and gain with voltage under a light intensity of 2.47 nW/cm^2. (g), (h) Variations of responsivity and gain with light intensity at 15 V. (i), (j) Time-resolved response of the photodetector illuminated by 405-nm light pules at 5 s intervals at 15 V.

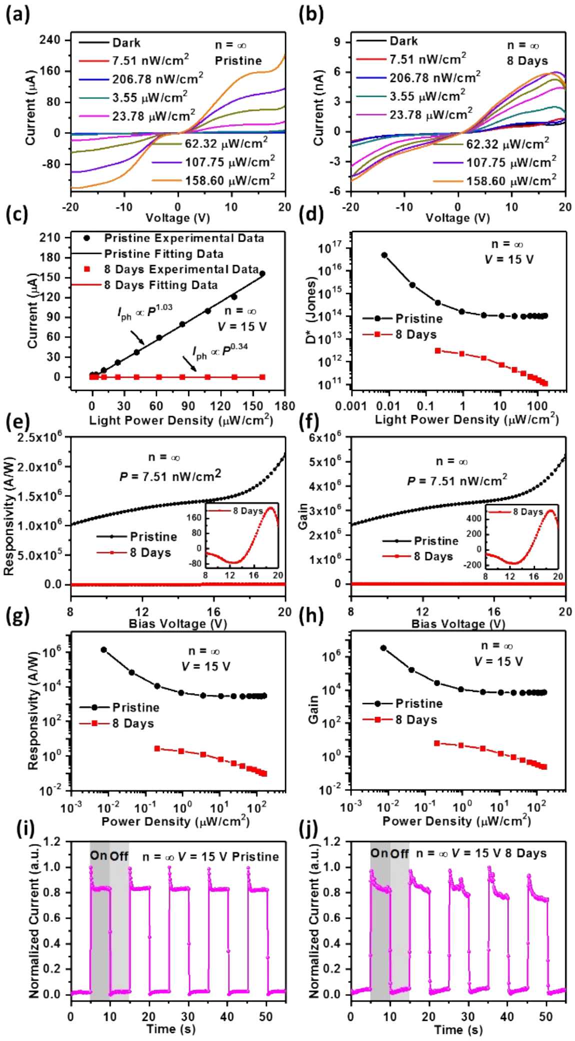

Fig. S13 Device charateristics of the pristine $MAPbBr_3$ perovskite photodetector and after being placed in an atmospheric environment with a humidity of 60% for 8 days. (a), (b) *I-V* characteristics in the dark and under 405-nm light illumination at various power intensities. (c), (d) Variations of photocurrent and specific detectivity with light intensity at 15 V. (e), (f) Variations of responsivity and gain with voltage under a light intensity of 2.47 nW/cm^2. The insets in (e), (f) show the magnified curves of responsivity and gain versus voltage after aging. (g), (h) Variations of responsivity and gain with light intensity at 15 V. (i), (j) Time-resolved response of the photodetector illuminated by 520-nm light pules at 5 s intervals at 15 V.

Table S1 Amount of each starting material for preparing the $(PEA)_2(MA)_{n-1}Pb_nBr_{3n+1}$ (n = 1, 3, 5, ∞) perovskite microcrystals according to stoichiometric ratios.

n	Perovskite	$PbBr_2$ concentration	MABr concentration	PEABr concentration
1	$(PEA)_2PbBr_4$	1 mmol/ml (367 mg/ml)	0	2 mmol/ml (404 mg/ml)
3	$(PEA)_2(MA)_2Pb_3Br_{10}$	1 mmol/ml (367 mg/ml)	0.67 mmol/ml (74.7 mg/ml)	0.67 mmol/ml (134.7 mg/ml)
5	$(PEA)_2(MA)_4Pb_5Br_{16}$	1 mmol/ml (367 mg/ml)	0.8 mmol/ml (89.6 mg/ml)	0.4 mmol/ml (80.8 mg/ml)
∞	$MAPbBr_3$	1 mmol/ml (367 mg/ml)	1 mmol/ml (112 mg/ml)	0

Table S2 Device performance parameters of the pristine photodetectors based on the $(PEA)_2(MA)_{n-1}Pb_nBr_{3n+1}$ (n = 1, 3, 5 ∞) perovskite microcrystals and after being placed in an atmospheric environment with a humidity of 60% for 8 days at 15 V.

n	Perovskite (days)	Rise Time (ms)	Decay Time (ms)	Responsivity (A/W)	Detectivity (Jones)	Gain
1	$(PEA)_2PbBr_4$ (p)	179.5	150.9	5.70	3.50×10^{13}	17.43
1	$(PEA)_2PbBr_4$ (8)	185.2	120.1	11.22	5.09×10^{13}	34.33
3	$(PEA)_2(MA)_2Pb_3Br_{10}$ (p)	149.9	369.6	351.78	2.56×10^{14}	1.16×10^{3}
3	$(PEA)_2(MA)_2Pb_3Br_{10}$ (8)	129.1	188.1	620.81	5.74×10^{14}	1.90×10^{3}
5	$(PEA)_2(MA)_4Pb_5Br_{16}$ (p)	358.4	589.8	182.63	2.51×10^{14}	5.58×10^{2}
5	$(PEA)_2(MA)_4Pb_5Br_{16}$ (8)	66.8	66.7	364.34	4.21×10^{14}	1.11×10^{3}
∞	$MAPbBr_3$ (p)	66.4	132.4	1.40×10^{6}	4.92×10^{16}	3.34×10^{6}
∞	$MAPbBr_3$ (8)	135.0	150.7	-	-	-

*p represents pristine; 8 represents 8 days.